# Impedance method for detecting HIV-1 protease and screening for its inhibitors using ferrocene-peptide conjugate/Au nanoparticle/single-walled carbon nanotube modified electrode

Mahmoud, Khaled A.; Luong, John H. T.



**Publisher's version / Version de l'éditeur:**
http://dx.doi.org/10.1021/ac801174r
*Analytical Chemistry, 80, 18, pp. 7056-7062, 2008-09-15*

*Anal. Chem.* **2008,** *80,* 7056–7062

# Impedance Method for Detecting HIV-1 Protease and Screening For Its Inhibitors Using Ferrocene−Peptide Conjugate/Au Nanoparticle/ Single-Walled Carbon Nanotube Modified Electrode

**Khaled A. Mahmoud[†] and John H. T. Luong*[,†,‡]**

*Biotechnology Research Institute, National Research Council Canada, Montreal, Quebec, Canada H4P 2R2, and Department of Chemistry, University College Cork, Cork, Ireland*



**A highly sensitive screening assay based on electrochemical impedance spectroscopy (EIS) has been developed for detecting HIV-1 protease (PR) and subsequent evaluation of its corresponding inhibitors at picomolar levels. The assay format was based on the immobilization of the thiol terminated ferrocene(Fc)−pepstatin conjugate on a single-walled carbon nanotube/gold nanoparticle (SWCNT/ AuNP) modified gold electrode. The alteration of the interfacial properties of electrodes upon HIV-1 PR and Fc−pepstatin conjugate interaction was traced by EIS. On the basis of the charge transfer resistance data obtained and using a mixed kinetic and diffusion model, this procedure was capable of detecting picomolar HIV-1 PR owing to the specific binding of this enzyme to Fc modified pepstatin. A competitive inhibition assay format was then performed using four potent HIV-1 PR inhibitors. The estimated inhibition constant ($K_i$) attested that lopinavir/ ritonavir ($K_i = 20 \pm 3$ pM) and saquinavir ($K_i = 57 \pm 8$ pM) even at 10 pM competed strongly with pepstatin for effective binding to HIV-1 PR. Indinavir ($K_i = 630 \pm 22$ pM) only competed well with pepstatin at a much higher concentration (1 nM). No significant inhibitory effect was observed for the fosamprenavir ($K_i = 11 \pm 0.5$ nM) as expected from this pro-drug. Such results agreed well with the values reported in the literature. This assay format is a definite asset for the expedited development of effective HIV-1 PR inhibitors with low molecular weights.**

The nucleotide sequence of the HIV-1 genome[1] reveals that the HIV-1 virus encodes an aspartic protease (HIV-1 PR), an essential enzyme for virion assembly and maturation. The enzyme can be inactivated by mutation or chemical inhibition, leading to the production of immature, noninfectious viral particles.[2−4] HIV-1 PR is inhibited by pepstatin, a classical inhibitor for aspartic proteases.[4,5] Since the elucidation of the crystal structures of native HIV-1 PR,[6,7] protease inhibitors have become a new class of medications used to treat or prevent infection by HIV. To date, the U.S. Food and Drug Agency (FDA) has approved several HIV-1 PR inhibitors for HIV/AIDS treatment. Although treatment with these inhibitors in multidrug regiments has significantly reduced viral load as well as mortality, a single amino acid change within HIV-1 PR can render it invisible to an inhibitor. The high mutation rate of HIV-1 PR together with serious side effects such as lipodystrophy, hyperlipidemia, and insulin resistance[8,9] has remained problematic. Hence, the search for new generations of HIV-1 PR inhibitors is essential for prolonged antiviral therapy.

Methods for assaying HIV protease have been developed both in vitro and in vivo, such as employing polyprotein or oligopeptide substrates, or the utilization of gel electrophoresis, or high performance liquid chromatography for ascertaining the presence of cleavage products.[10−12] Other screening methods involve the coexpression of HIV-1 PR and a biochemical marker, e.g., enhanced green fluorescent protein, in which this marker protein is cleaved or degraded by HIV-1 PR, resulting in a loss/attenuation of the marker activity.[13−16]Despite their advantages, such screen-

* To whom correspondence should be addressed. E-mail: john.luong@cnrc-nrc.gc.ca or j.luong@vcc.ie.
† National Research Council Canada.
‡ University College Cork.

(1) Ratner, L.; Haseltine, W.; Patarca, R.; Livak, K. J.; Starcich, B.; Josephs, S. F.; Doran, E. R.; Rafalski, J. A.; Whitehorn, E. A.; Baumeister, K.; Ivanoff, L., Jr.; Pearson, M. L.; Lautenberger, J. A.; Papas, T. S.; Ghrayeb, J.; Chang, N. T.; Gallo, R. C.; Wong-Staal, F. *Nature* **1985**, *313*, 277–284.
(2) Kohl, N. E.; Emini, E. A.; Schleif, W. A.; Davis, L. J.; Heimbach, J. C.; Dixon, R. A.; Scolnick, E. M.; Sigal, I. S. *Proc. Natl. Acad. Sci. U.S.A.* **1988**, *85*, 4686–4690.
(3) McQuade, T. J.; Tomasselli, A. G.; Liu, L.; Karacostas, B.; Moss, B.; Sawyer, T. K.; Heinrikson, R. L.; Tarpley, W. G. *Science* **1990**, *247*, 454–456.
(4) Seelmeier, S.; Schmidt, H.; Turk, V.; von der Helm, K. *Proc. Natl. Acad. Sci. U.S.A.* **1988**, *85*, 6612–6616.
(5) Richards, A. D.; Roberts, R.; Dunn, B. M.; Graves, M. C.; Kay, J. *FEBS Lett.* **1989**, *247*, 113–117.
(6) Lapatto, R.; Blundell, T.; Hemmings, A.; Overington, J.; Wilderspin, A. F.; Wood, S.; Merson, J. R.; Whittle, P. J.; Danley, D. E.; Geoghegan, K. F.; Hawrylik, S. J.; Lee, S. E.; Scheld, K. G.; Hobart, P. M. *Nature* **1989**, *342*, 299–302.
(7) Navia, M. A.; Fitzgerald, P. M.; McKeever, B. M.; Leu, C. T.; Heimbach, J. C.; Herber, W. K.; Sigal, I. S.; Darke, P. L.; Springer, J. P. *Nature* **1989**, *337*, 615–620.
(8) Carr, A. *Nat. Rev. Drug Discovery* **2003**, *2*, 624–634.
(9) Nolan, D. *Drugs* **2003**, *63*, 2555–2574.
(10) Molla, A.; Vasavanonda, S.; Kumar, G.; Sham, H. L.; Johnson, M.; Grabowski, B.; Denissen, J. F.; Kohlbrenner, W.; Plattner, J. J.; Leonard, J. M.; Norbeck, D. W.; Kempf, D. J. *Virology* **1998**, *250*, 255–262.
(11) Krausslich, H. G.; Ingraham, R. H.; Skoog, M. T.; Wimmer, E.; Pallai, P. V.; Carter, C. A. *Proc. Natl. Acad. Sci. U.S.A.* **1989**, *86*, 807–811.
(12) Gillim, L.; Gusella, G. L., Jr.; Marras, D.; Klotman, M. E.; Cara, A. *Clin Diag. Lab Immunol.* **2001**, *8*, 437–440.
(13) Hu, K.; Clement, J. F.; Abrahamyan, L.; Strebel, K.; Bouvier, M.; Kleiman, L.; Mouland, A. J. *J. Virol. Methods* **2005**, *128*, 93–103.
(14) Lindsten, K.; Uhlikova, T.; Konvalinka, J.; Masucci, M. G.; Dantuma, N. P. *Antimicrob. Agents Chemother.* **2001**, *45*, 2616–2622.



10.1021/ac801174r CCC: $40.75 
Published on Web 08/16/2008

ing systems can only detect the inhibitor in the micromolar range whereas only a nanomolar or lower range of such drugs can be used in HIV-1 therapy.[13] Hence, there is a critical need for high throughput and sensitive protocols for detecting protease activity and/or screening novel protease inhibitors.

Electrochemical impedance spectroscopy (EIS) is a very efficient and highly sensitive electroanalytical approach that can provide direct detection of immunospecies by measuring the change of impedance. Besides its simplicity and ease of operation, EIS provides a nondestructive means for the characterization of the electrical properties at biological interfaces,[17,18] which makes it extremely attractive for electrochemical biosensing methods.[19−22] Extensive work has been reported on DNA sensing and aptamer-based protein recognition assays.[23] Hitherto, this detection approach has not been developed or widely used to assay drug efficacy.

This paper describes an ultrasensitive impedance procedure for detecting HIV-1 PR and screening its potent inhibitors using ferrocene (Fc)−pepstatin-modified surfaces. Of particular interest is the use of pepstatin, a hexapeptide (Iva-Val-Val-Sta-Ala-Sta) with an unusual amino acid, statine or (3 *S*,4 *S*)-4-amino-3-hydroxy-6-methylheptanoic acid. Pepstatin was first isolated from *Actinomyces*[24] because of its ability to inhibit pepsin at low concentrations.[25] The gold electrode surface is modified with thiolated single-walled carbon nanotube (SWCNT)/gold nanoparticle (AuNP). Thiol-terminated Fc−pepstatin is self-assembled on such surfaces as the sensing probe. The interaction and binding between the Fc−pepstatin-modified substrates and HIV-1 PR is studied by EIS. HIV-1 protease when forming a complex with a potent inhibitor will no longer bind to the pepstatin-modified electrode and provokes reduced or no signal response. Differential pulse voltammetry (DPV) was also performed to support the results obtained by EIS.

## EXPERIMENTAL SECTION

**Reagents and Materials.** HIV-1 PR recombinant expressed in *Escherichia coli* (25 $\mu$g), human serum albumin (HSA), and human male serum were purchased from Sigma (St. Louis, MO). DTT (± threo-2,3-dihydroxy-1,4-butanedithiol) was obtained from Fluka. Fc-conjugated pepstatin (Cys-(NH-Pro$_4$-C(O)-Fc-C(O)-Val$_2$-Sta-Ala-Sta-OH)$_2$ was prepared as described before.[26] Single-walled carbon nanotubes (SWCNTs) (diameter of 1 nm, purity of CNTs >90 wt %; length, 5−30 $\mu$m; specific surface area, 407 m$^2$/g; electrical conductivity, $>10^{-2}$ S/cm) were purchased from Carbon Nanotechnology (Houston, TX). An amount of 100 mg of the pure substances, indinavir sulfate (Crixivan) and saquinavir mesylate (Invirase), were donated by Merck and Roche, respectively. The other two HIV-1 drugs Kaltera (yellow tablets with 200 mg of lopinavir and 50 mg of ritonavir, Abbott), and Telzir (pink tablets with 700 mg of fosamprenavir calcium, GlaxoSmithKline) were obtained from Dr. Chris Tsoukas, an HIV specialist of the McGill University Health Center (Montreal, QC, Canada). The chemical structure and solubility data of the above HIV-1 PR inhibitors are given in Table S1 (Supporting Information). Other FDA approved HIV-1 PR inhibitors were not available to us during the course of this study.

**Instrumentation.** Cyclic voltammetry (CV), electrochemical impedance spectroscopy (EIS), and amperometric measurements were performed using an electrochemical analyzer coupled with a picoampere booster and a Faraday cage (CHI 760B, CH Instruments, Austin, TX). A Pt wire (Aldrich, 99.9% purity, 1 mm diameter) and an Ag/AgCl, 3 M NaCl (BAS, West Lafayette, IN) electrode were used as counter and reference electrodes, respectively. Scanning electron microscope (SEM) (Hitachi, S-2600 N, Tokyo, Japan) operating in high vacuum mode with an acceleration voltage of 10−24 kV and a working distance of 3−15 mm, depending on the sample was used to analyze the morphology of SWCNTs before and after different modification steps. AFM measurements were carried out by a Nanoscope IV system (Digital Instruments-Veeco, Santa Barbara, CA), operating in air in the tapping mode. Silicon AFM probes with a cantilever length of 125 mm and drive frequencies of 235−255 kHz were employed for imaging. The image scan speed was 0.50 Hz at 512 lines/scan. All height measurements and size distribution were obtained from the analysis of the software package of the instrument.

**Preparation of Modified Electrodes.** Gold disk electrodes (3 mm in diameter, BAS, West Lafayette, IN) were carefully polished with polishing paper (grid 2000) and subsequently with alumina until a mirror finish was obtained. The electrodes were sonicated for 5 min to remove the alumina residues followed by thorough rinsing with water and ethanol. The electrodes were then cleaned electrochemically by cyclic voltammetry between 0 and +1.4 V versus Ag/AgCl at 100 mVs$^{-1}$ in 0.5 M $H_2SO_4$, until a stable CV profile was obtained. The preparation of SWCNT/AuNP modified gold electrodes and immobilization of the peptide films were described in detail elsewhere.[27] In brief, the electrodes were immersed in thiol-terminated Fc−pepstatin conjugate prepared in 5% (by volume) acetic acid in ethanol at a concentration of ~1 mM for 12 h. A 20 nM HIV-1 PR stock solution was prepared in 0.1 M sodium acetate, pH 7.4, containing 2 mM EDTA, 1 mM DTT, and 10% DMSO and was incubated at 23 °C for 1 h prior to the measurement. The activated enzyme was kept on ice.



(15) Cheng, T. J.; Brik, A.; Wong, C. H.; Kan, C. C. *Antimicrob. Agents Chemother.* **2004**, *48*, 2437–2447.
(16) Fuse, T.; Watanabe, K.; Kitazato, K.; Kobayashi, N. *Microbes Infect.* **2006**, *8*, 1783–1789.
(17) Chen, H.; Jiang, J. H.; Huang, Y.; Deng, T.; Li, J. S.; Shen, G. L.; Yu, R. Q. *Sens. Actuators, B* **2006**, *117*, 211–218.
(18) Chen, X.; Wang, Y.; Zhou, Z.; Yan, W.; Li, X.; Zhu, J.-J. *Anal. Chem.* **2008**, *80*, 2133–2140.
(19) Dijksma, M.; Kamp, B.; Hoogvliet, J. C.; van Bennekom, W. P. *Anal. Chem.* **2001**, *73*, 901–907.
(20) Sadik, O. A.; Xu, H.; Gheorghiu, E.; Andreescu, D.; Balut, C.; Gheorghiu, M.; Bratu, D. *Anal. Chem.* **2002**, *74*, 3142–3150.
(21) (a) Darain, F.; Park, D. S.; Park, J. S.; Shim, Y. B. *Biosens. Bioelectron.* **2004**, *19*, 1245–1252. (b) Wang, M. J.; Wang, L. Y.; Wang, G.; Ji, X. B.; Bai, Y. B.; Li, T. J.; Gong, S. Y.; Li, J. H. *Biosens. Bioelectron.* **2004**, *19*, 575–582.
(22) Cai, W.; Peck, J. R.; van der Weide, D. W.; Hamers, R. J. *Biosens. Bioelectron.* **2004**, *19*, 1013–1019.
(23) (a) Xu, D.; Xu, D.; Yu, Z.; He, W.; Ma, Z. *Anal. Chem.* **2005**, *77*, 5107–5113. (b) Li, C.-Z.; Liu, Y.; Luong, J. H. T. *Anal. Chem.* **2005**, *77*, 478–485. (c) Cai, H.; Lee, T.; Hsing, I.-M. *Sens. Actuators, B* **2006**, *114*, 433–437. (d) Li, C.-Z.; Long, Y.-T.; Lee, J.; Kraatz, H.-B. *J. Phys. Chem. B* **2003**, *107*, 2291–2296.
(24) Umezawa, H.; Aoyagi, T.; Morishima, H.; Matsuzaki, M.; Hamada, M. *J. Antibiot.* **1970**, *23*, 259–262.
(25) Marciniszyn, J.; Hartsuck, J. A.; Tang, J. *J. Biol. Chem.* **1976**, *251*, 7088–7094.
(26) Kerman, K.; Mahmoud, K. A.; Kraatz, H.-B. *Chem. Commun.* **2007**, 3829–3831.
(27) Mahmoud, K. A.; Hrapovic, S.; Luong, J. H. T. *ACS Nano* **2008**, *2*, 1051–1057.

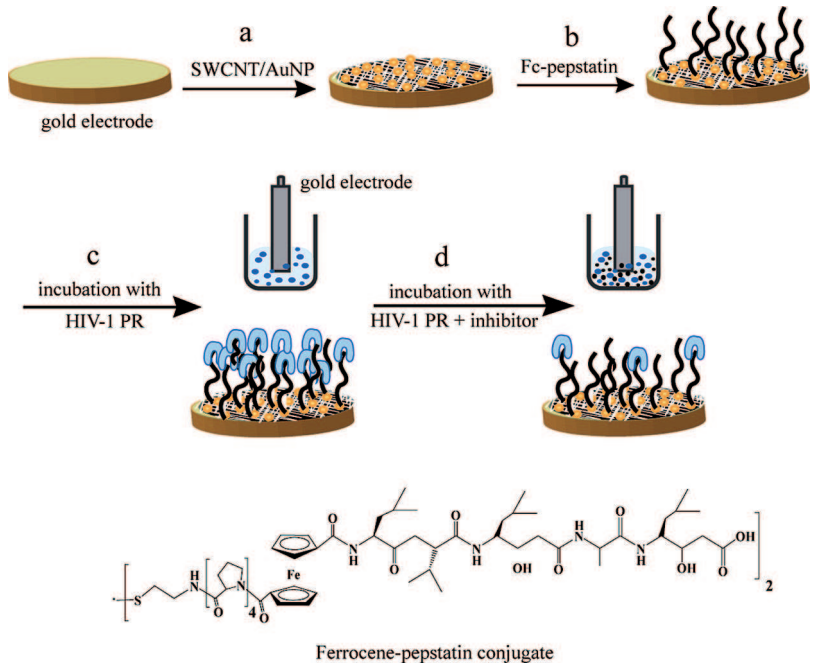


**Figure 1.** Schematic illustration for the preparation of ferrocene−pepstatin conjugate/thiolated single-walled carbon nanotube (SWCNT) and gold nanoparticle (AuNP) modified electrodes and their use for detecting HIV-1 protease and the subsequent assay of HIV-1 protease inhibitors.



Subsequent dilutions of the enzyme were prepared by using the assay buffer. The peptide modified electrodes were incubated with different HIV-1 PR concentrations for 1 h and washed twice with the assay buffer and deionized water, respectively. Control experiments were carried out with 75 $\mu$M HSA with and without HIV-1 PR.

For SEM and AFM imaging, silicon-supported gold films for AFM imaging were purchased from Platypus Technologies LLC (Madison, WI). The topical thickness of Au was ~1000 Å. Before each experiment, the electrodes were cleaned by electrochemical treatment. After the modification of the gold surface with SWCNT/AuNP and Fc−pepstatin, the resulting surface was incubated in a buffer containing 10 pM HIV-1 PR for 1 h followed by rinsing with the buffer solution and distilled water, respectively. The prepared surface was dried with nitrogen and immediately used for imaging.

**Drug Assay.** For the drug assay experiment, the pure substance of clinical inhibitors saquinavir and indinavir were dissolved in the HIV-1 PR buffer solution (pH 7.4) and subsequent dilutions (10, 100, and 1000 pM) were prepared. Lopinavir/ritonavir and fosamprenavir were prepared by dissolving the clinical capsules in the same buffer. The effective concentration was estimated based on the formulation of the capsules as described in Table S1 (Supporting Information). The electrodes were then incubated in four different solutions with a fixed enzyme concentration (10 pM), and increasing concentrations of the desired inhibitor in the following ratios: (HIV-1 PR/inhibitor) (1:0, 1:1, 1:10, and 1:100). Differential pulse voltammetry (DPV) and electrochemical impedance spectroscopy (EIS) measurement were performed in a pH 7.4 buffer medium. A 1:1 mixture of 5.0 mM $Fe(CN)_6^{3-/4-}$ was used as the redox probe in all impedance measurements. All measurements were performed in a 1 mL-electrochemical cell, which had been purged for 10 min before each measurement. The modified electrodes were incubated with the inhibitor for 30 min before each measurement to allow the system to equilibrate. For EIS, impedance was measured at the bias potential of 0.45 V versus Ag/AgCl and superimposed on a sinusoidal potential modulation of ±5 mV. The frequency window used for impedance measurements ranged from 0.1 Hz to 100 kHz. The impedance data for the SWCNT/Au NP, Fc−pepstatin conjugate, and HIV-1 PR modified gold electrodes was simulated by CHI 760B program (CH Instruments, Austin, TX) and analyzed using the ZSimpWin software (Princeton Applied Research). From repeated measurements, the error in $R_s$ and $R_{ct}$ is estimated to be ±35Ω. In all impedance spectra, symbols represent the experimental raw data, and the solid lines are the fitted curves. Schematic illustration of the immobilization process of the Fc−pepstatin conjugate onto the SWCNT/AuNP modified gold electrode and competitive inhibition assays for HIV-1 PR in the absence and presence of the HIV-1 PR inhibitors is described in Figure 1.

## RESULTS AND DISCUSSION

**Electrode Preparation and Characterization.** A thin film of prethiolated SWCNTs was coated on the electrode surface, then AuNPs were formed on the thiol terminals by electrochemical deposition from 0.5 M $H_2SO_4$ solution containing 5 mM $HAuCl_4$. The monolayer of the cystamine containing the Fc−pepstatin conjugate was formed on the SWCNT/AuNP modified electrode surface through Au−S self-assembly interaction. The formation of the SWCNT/AuNP composite was confirmed by SEM and AFM as shown in Figure 2. After incubation of the modified electrode in a buffer containing 10 pM HIV-1 PR, SEM and AFM show an interesting pattern of well separated protein clusters. The AFM topographic image (Figure 2B) clearly shows that the protein clusters were positioned well above the SWCNT/AuNP/Fc−pepstatin film. The well shaped surface morphology could be attributed to various protein orientations or the formation of a protein multilayer on the background surface, indicative of HIV-1 PR interaction with the Fc−pepstatin film.

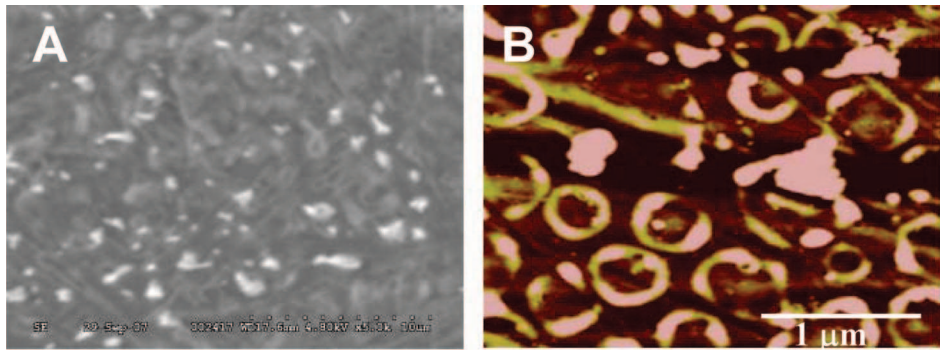


**Figure 2.** (A) SEM micrograph (5000×) and (B) AFM micrograph of the SWCNT/AuNP/Fc−pepstatin film after incubation with 10 pM of HIV-1 PR. The micrographs were taken in situ for the dried samples after successive washing with the buffer solution and deionized water. The figures show the pattern of uniform and well separated protein aggregates, which are positioned above the peptide modified surface as evident from AFM imaging.

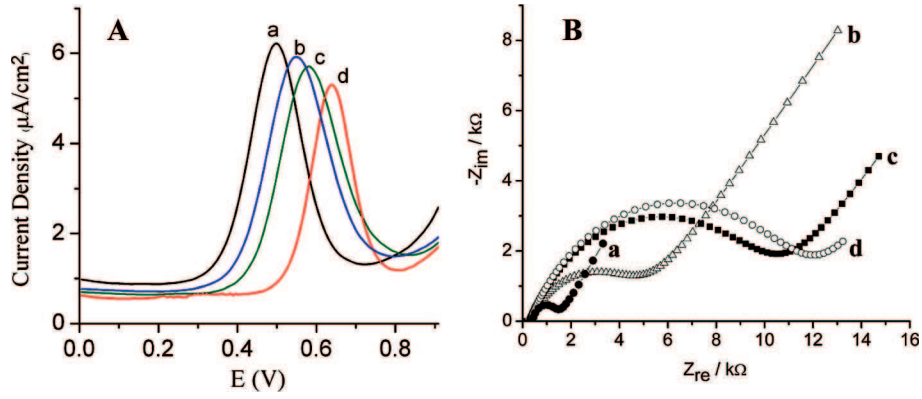


**Figure 3.** (A) Differential pulse voltammograms of Fc−pepstatin/SWCNT/AuNP modified gold electrodes in the presence of different concentrations of HIV-1 PR (pM): (a) 0, (b) 10, (c) 100, and (d) 1000. Ag/AgCl was used as reference at 100 mV $s^{-1}$. The assay buffer consisted of 0.1 M sodium acetate, 2 M $NaClO_4$, 1 mM EDTA, 1 mM DTT, and 10% DMSO, pH 7.4. The $E^{\circ}$ of the $Fc/Fc^{+}$ couple under the experimental conditions was 448 (±5) mV. (B) The Nyquist plot for the Faradic impedance in a pH 7.4 buffer with $Fe(CN)_6^{3-/4-}$ as the redox probe for the CNT/AuNP modified gold electrode: (a) before modification, (b) after modification with Fc−pepstatin, (c) after 1 h-incubation with 10 pM HIV-1 PR, and (d) after 1 h-incubation with 100 pM HIV-PR. The impedance spectra were recorded from 0.1 Hz to 100 kHz at the formal potential of the redox couple. The amplitude of the alternate voltage was 5 mV. The symbols represent the experimental data, and the solid lines are the fitted curves using the equivalent circuit.

**Electrochemical Detection of HIV-1 PR.** The formation of a stable monolayer of the Fc−pepstatin conjugate as the recognition element on the SWCNT/Au NP modified electrode and its interaction with HIV-1 PR was confirmed by DPV (Figure 3A). The position of the Fc group in close proximity to the electrode surface allowed for monitoring any change in the electrode potential before and after the interaction with increasing concentration of the enzyme. The films displayed an oxidation peak at $E_{ox} = 0.495 \pm 0.005$ at 0.1 V/s vs Ag/AgCl. Upon the selective binding of HIV-1 PR to the surface bound inhibitory peptide (Fc−pepstatin), a shift to higher potential together with a decrease in the peak current intensity was observed. This change could be attributed to blocking the penetration of the supporting electrolyte to the electrode surface, thereby decreasing its ability to oxidize the Fc moiety.[27] Even at 10 pM enzyme concentration (Figure 3A), a well pronounced shift in the formal potential ($\Delta E$ = 55 mV) was observed in response to the binding of this enzyme on the Fc−pepstatin modified electrode.

Electrochemical impedance spectroscopy (EIS) further confirmed the binding event on the electrode surface. Impedance measurement, using 1 mM $Fe(CN)_6^{3-/4-}$ as the redox probe, shows a typical Nyquist plot for the CNT/AuNP modified gold electrode.

**Scheme 1. An Equivalent Circuit Model for Mixed Kinetic and Diffusion Control[a]**

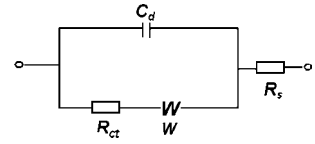


[a] $R_s$, solution resistance; $C_d$, double-layer capacitance; $R_{ct}$, charge transfer resistance; and $W$, Warburg impedance.

The plot exhibited a semicircle near the origin at high frequencies followed by a linear tail with a slope of unity (Figure 3B). Others have described similar curves, and the data can be fitted adequately by the modified Randles circuit,[28] a well-known mixed kinetic and diffusion control model (Scheme 1). In brief, the monolayer can be treated as a resistor ($R_{ct}$) and capacitor in parallel ($C_d$), and the solution resistance is represented by a resistor ($R_s$). The Warburg impedance ($W$), arising from diffusion of the redox couple to and from the electrode, is noticeable at low frequencies.

(28) Patolsky, F.; Zayats, M.; Katz, B.; Willner, I. *Anal. Chem.* **1999**, *71*, 3171–3180.

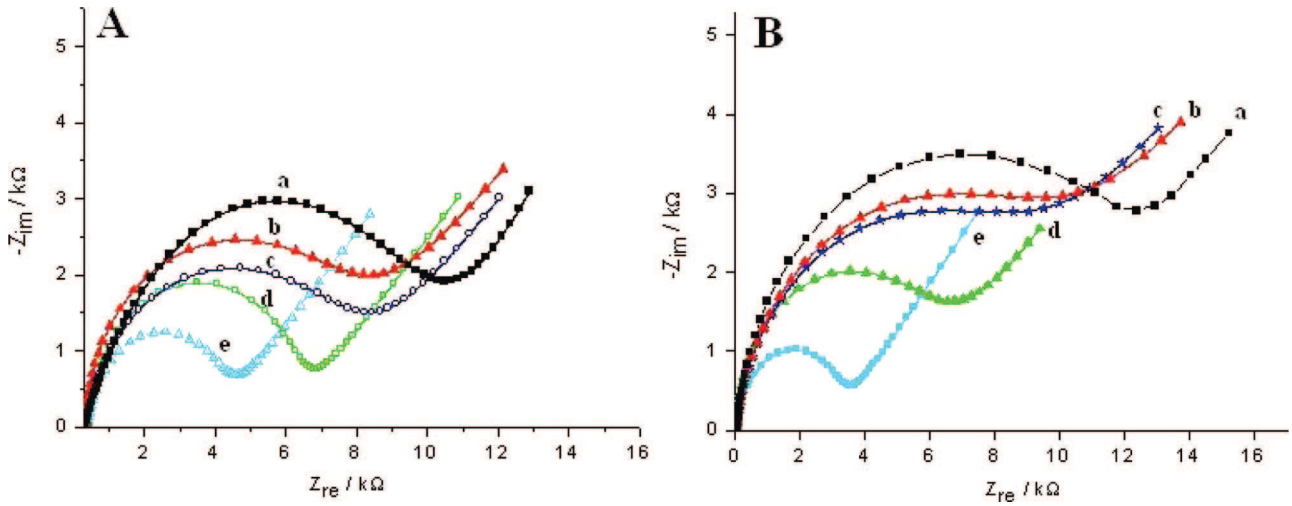


**Figure 4.** The Nyquist plot for the Faradic impedance in a pH 7.4 buffer with $Fe(CN)_6^{3-/4-}$ as the redox probe for the CNT/AuNP modified gold electrode after incubation with 10 pM HIV-1 PR in the presence of (A) saquinavir and (B) indinavir. HIV-1 PR/inhibitor ratios: (a) 1:0, (b) 1:1, (c) 1:10, (d) 1:100, and (e) 0:100. Other conditions were as described in Figure 3.



The equivalent circuit was used mainly to determine $C_d$ and $R_{ct}$ since $R_s$ and $W$ represent bulk properties of the electrolyte solution and diffusion of the applied redox probe, respectively, and are not sensitive to chemical transformation at the electrode interface. Any change in $C_d$ should be negligible compared to the change in $R_{ct}$. A redox-active probe is useful in this case, resulting in a well-defined charge transfer resistance $R_{ct}$. The binding event between a target analyte with its corresponding ligand will block the diffusion and passage of the redox probe to the active area of the detecting electrode. Consequently, $R_{ct}$ becomes increasingly high and can be used to monitor the binding event. Therefore $R_{ct}$ is the most directive and sensitive parameter that responds to changes on the electrode interface, as represented by the diameter of the semicircle in the Nyquist plot.[28]

A considerable increase in $R_{ct}$ was observed with the Fc−pepstatin/CNT/AuNP electrode compared to the CNT/AuNP modified electrode (4814 vs 19.6 Ω). Such behavior indicated that the electron transfer to the electrode was significantly reduced due to the binding of Fc−pepstatin to CNTs. The subsequent binding of HIV-1 PR (10 and 100 pM) to Fc−pepstatin provoked a further increase in $R_{ct}$ to 10 230 and 11 620 Ω, respectively. As expected, changes in $R_s$, $C_d$, and $W$ were insignificant compared to the change in $R_{ct}$ (Supporting Information, Table S2). The modified circuit also provided an excellent fit to the experimental data at both low and high frequency for the Fc−pepstatin/CNT/AuNP modified electrode and the subsequent binding event with HIV-1 PR (Figure 3B). The binding of only 10 pM of HIV-1 PR to the Fc−pepstatin/CNT/Au NP modified electrode provoked a significant change in $R_{ct}$. The Fc−pepstatin binding site became almost saturated since further increase in the HIV-1 PR concentration beyond this level only effected a slight increase in $R_{ct}$ (Supporting Information, Table S2). On the basis of this finding, the Fc−pepstatin/CNT/Au NP modified electrode together with 10 pM HIV-1 PR was used as a starting point for testing the selected HIV-1 PR inhibitors.

**Screening for HIV-1 PR Inhibitors.** A series of experiments was conducted to evaluate the response signal of the Fc−pepstatin/AuNP/CNT modified electrode, submerged in an assay buffer containing 10 pM HIV-1 PR and four different FDA approved HIV-1 PR inhibitors for the treatment of HIV-AIDS patients. The modified electrode when incubated with the enzyme in the presence of increasing concentration of the inhibitors reduced the amount of the enzyme available for binding to the Fc−pepstatin inhibitory sequence and therefore suppressed the resulting electrochemical signal. First, the two pure substances from two inhibitors, saquinavir and indinavir, were studied. Figure 4 illustrates the Faradic impedance change of the CNT/AuNP/Fc−pepstatin

**Table 1. Simulated Impedance Values of $R_{ct}$ of the CNT/AuNP/Fc-Pepstatin Modified Gold Electrode after Incubation with 10 pM HIV-1 PR and a Mixture Consisting of 10 pM HIV-1 PR and Saquinavir, Indinavir, Lopinavir/Ritonavir, or Fosamprenavir at Different Concentrations**

| | ratio/10 pM (HIV-1 PR/inhibitor) | | | | |
|---|---|---|---|---|---|
| $R_{ct}$/Ω | 1:0 | 1:1 | 1:10 | 1:100 | 0:100 |
| saquinavir | 10 781 | 5 731 | 2 571 | 618 | 20.1 |
| indinavir | 11 070 | 8 164 | 7 099 | 630 | 33.8 |
| lopinavir/ritonavir | 10 398 | 5 219 | 1 426 | 432 | 28.2 |
| fosamprenavir | 11 380 | 11 051 | 9 910 | 5 749 | 65.4 |

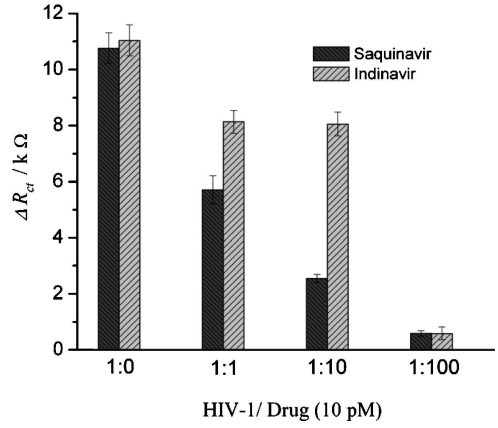


**Figure 5.** The change in the electron transfer resistance $\Delta R_{ct}$ in response to the indirect competitive inhibition assay of HIV-1 PR with saquinavir or indinavir. Other conditions were as described in Figure 3.

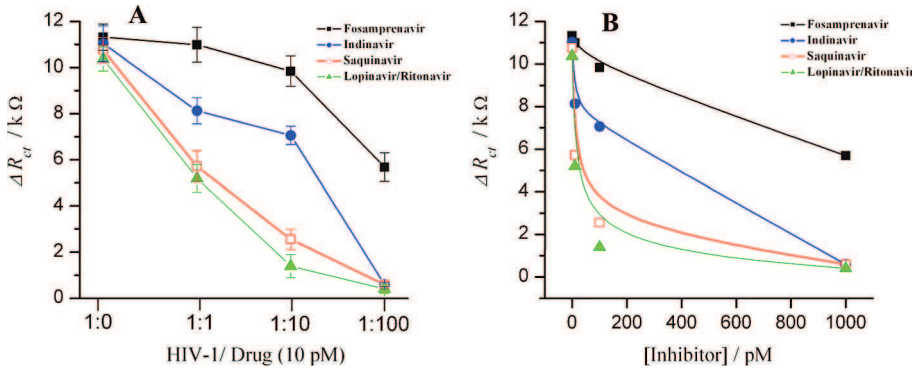


**Figure 6.** (A) The change in the charge transfer resistance $\Delta R_{ct}$ of the Fc−pepstatin/SWCNT/AuNP modified electrode in response to increasing concentrations of saquinavir, indinavir, lopinavir/ritonavir, or fosamprenavir. Other conditions were as described in Figure 3. (B) A replot of Figure 6A, $\Delta R_{ct}$ vs inhibition concentration for estimating the inhibition constant ($K_i$).



modified gold electrode in response to competitive inhibition of saquinavir and indinavir, respectively, for 10 pM HIV-1 PR. The following (HIV-1 PR/inhibitor) molar concentration ratios were used: 1:0, 1:1, 1:10, and 1:100. Saquinavir, the first approved drug by FDA, even at 10 pM competed with Fc−pepstatin for effective binding to HIV-1 PR, resulting in a significant decrease in $R_{ct}$ from 10 781 to 5 731 Ω (Table 1). Further increase in the concentration of saquinavir significantly decreased the value of $R_{ct}$. Notice that without HIV-1 PR, saquinavir even at 1 nM did not provoke any change in $R_{ct}$. A similar trend was also observed for indinavir (FDA approved in 1996) except that the resulting $R_{ct}$ value was appreciably higher compared to that of saquinavir, particularly at the concentration below 100 pM (Table 1). Other simulated values ($C_d$, $W$, and $R_s$) of the impedance model obtained for saquinavir and indinavir under different concentrations are found in Tables S3 and S4 (Supporting Information), respectively.

Figure 5 shows a comparison between saquinavir and indinavir which appeared to agree well with the inhibition data reported for the two inhibitors, i.e., the former is a stronger inhibitor than the latter. However, both the inhibitors' effect was equal at the high concentration (1 nM). Indinavir is much more water soluble than saquinavir (100 mg/mL or 140 mM vs 2.22 mg/mL or 2.89 mM, Table S1). However, this factor was not relevant since the inhibition assay was only performed up to 1 nM. The above two FDA approved inhibitors possess a critical hydroxyl group that hydrogen bonds to the carboxyl groups of the catalytically active aspartic acids of HIV-1 PR. It has been known that indinavir is potent and competitively inhibits HIV-1PR with a $K_i$ value of 0.52 nM.[29] A similar value (0.571 ± 0.143 nM) was reported for this inhibitor, compared to 67.3 ± 5.2 pM for saquinavir.[30]

Two FDA approved commercial drugs tested in this study, lopinavir/ritonavir and fosamprenavir, were dissolved in the buffer solution and examined in situ without any further purification. The interpretation of the inhibition data for lopinavir/ritonavir was somewhat difficult since this Keletra capsule contains 133.3 mg of lopinavir, 33.3 mg of ritonavir, and other inactive ingredients (Table S1, Supporting Information). Neglecting the inhibition or activation effect of such inactive ingredient on the enzyme, this formulation effectively inhibited HIV-1 PR and compared well with saquinavir. At 10 pM, combined liponavir/ritonavir competed with Fc−pepstatin for effective binding to HIV-1 PR, resulting in a significant decrease in $R_{ct}$ from 10 398 to 5 219 Ω. The value of $R_{ct}$ was only 432 Ω at 1 nM liponavir/ritonavir (Table 1). The $K_i$ value for lopinavir and ritonavir was reported to be 17.5 ± 6.9 and 100 ± 17 pM, respectively.[30] Telzir tablets contain 700 mg of fosamprenavir calcium, equivalent to approximately 600 mg of amprenavir and several other inactive ingredients. The inhibitory constant ($K_i$) for amprenavir is 0.6 nM whereas fosamprenavir is not considered as a potent inhibitor for HIV-1 PR.[29] Hence, fosamprenavir was used as a control in this study. As expected, even at 1 nM, fosamprenavir did not bind to HIV-1 PR, compared to the other three inhibitors (Figure 6). Below 100 pM, fosamprenavir did not provoke any significant change in $R_{ct}$ (Table 1). The data of Figure 6 were then used to estimate the apparent inhibitory constant of the above HIV-1 PR inhibitors using exponential regression analysis. Lopinavir/ritonavir coformulation performed very well and exhibited the highest binding potency with a $K_i$ value of 20 ± 3 pM, comparable to the literature value of 17.5 ± 6.9 pM for liponavir and 100 ± 17 pM for ritonavir, respectively.[30] Sequinavir was also confirmed as a potent inhibitor for HIV-1 PR with a $K_i$ value of 57 ± 8 pM, comparing well to the reported value of 67.3 ± 5.2 pM.[30] To a lesser extent, indinavir inhibited HIV-1 PR with a $K_i$ constant of 630 pM, comparable to the literature values[30] of 520 ± 22 and 571 ± 143 pM. Fosamprenavir, on the other hand, showed no significant effect on HIV-1 PR with a $K_i$ value of above 10 nM. No significant change in $R_{ct}$ was noted even at 100 pM level (Table 1). However, this point was not important with respect to its use in HIV-1 PR therapy since fosamprenavir will be rapidly metabolized and hydrolyzed to amprenavir in the body, a more potent HIV-1 PR inhibitor.[31]

Although EIS has been used to detect HIV-1 PR and its corresponding inhibitors, other electrochemical techniques including cyclic voltammetry should be applicable as demonstrated by our recent publication.[27] However, impedance detection still hold the advantage of achieving the sensitivity required for practical applications in medicine, gene analysis, food industry, and environmental analysis.

In order to validate this point and gain further support for impedance inhibition assays, measurements were also carried out

(29) Abbenante, G.; Fairlie, D. P. *Med. Chem.* **2005**, *1*, 71–104.
(30) Cihlar, T.; He, G.-X.; Liu, X.; Chen, J. M.; Hatada, M.; Swaminathan, S.; McDermott, M. J.; Yang, Z.-Y.; Mulato, A. S.; Chen, X.; Leavitt, S. A.; Stray, K. M.; Lee, W. A. *J. Mol. Biol.* **2006**, *363*, 635–647.
(31) Aruksakunwong, O.; Promsri1, S.; Wittayanarakul, K.; Nimmanpipug, P.; Lee, V. S.; Wijitkosoom, A.; Sompornpisut, P.; Hannongbua, S. *Curr. Comput.-Aided Drug Des.* **2007**, *3*, 201–213.

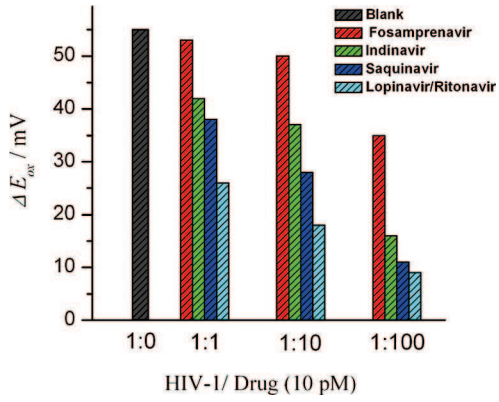


**Figure 7.** The change in the peak potential $\Delta E_{ox}$ of the modified electrode using 10 pM of HIV-1 PR in the presence of increasing inhibitor concentrations. (HIV-1 PR/inhibitor) ratios: (1:0, 1:1, 1:10, 1:100). Ag/AgCl was used as the reference electrode at 100 mV $s^{-1}$. The blank was the HIV-1 PR binding in the absence of the inhibitors. The assay buffer consisted of 0.1 M sodium acetate, 2 M $NaClO_4$, 1 mM EDTA, 1 mM DTT, and 10% DMSO, pH 7.4. The $E^{\circ}$ of the Fc/Fc+ couple under the experimental conditions was 448 (±5) mV.

involving DPV on the Fc−pepstatin modified electrode. DPV was able to discriminate between the potency of the four inhibitors by monitoring the resulting shift in the peak potential of the ferrocene group of the Fc−pepstatin/SWCNT/AuNP electrode due to competitive binding between the inhibitor and Fc−pepstatin for HIV-1 PR. Again, lopinavir/ritonavir resulted in the highest signal reduction followed by saquinavir and indinavir whereas an insignificant inhibitory effect was noted for fosamprenavir (Figure 7).

In brief, this study has demonstrated for the first time the use of nanomaterials in impedance spectroscopy for detecting HIV-1 protease and subsequent evaluation of the enzyme inhibitors at picomolar levels. Thiolated single-walled carbon nanotubes together with gold nanoparticles and a ferrocene-conjugate serve as sensitive enhancer tools in this assay format. On the basis of its applicability for evaluation of low-molecular weight compounds, this technique is a definite asset for the expedited development of effective HIV-1 PR inhibitors. This strategy might be extended for the sensing of other interfacial interactions such as enzyme−DNA, antibody−antigen, and cell−receptor.

## ACKNOWLEDGMENT

We thank Chris Tsoukas, M.D. of the McGill University Health Center, Montreal, Quebec, Canada, for the two anti HIV-1 protease drugs: Kaletra and Telzir. Pure indinavir sulfate and saquinavir mesylate were kindly donated by Merck and Roche, respectively. Acknowledgment is also extended to S. Hrapovic and Y. Liu for obtaining SEM and AFM images and K. B. Male of the National Research Council Canada, Biotechnology Research Institute, Montreal, Canada, for valuable discussion.

## SUPPORTING INFORMATION AVAILABLE

Additional information as noted in text. This material is available free of charge via the Internet at http://pubs.acs.org.

Received for review June 10, 2008. Accepted July 18, 2008.

AC801174R